Electronic Materials Letters, Vol. 9, No. 2 (2013), pp. 187-193
DOI: 10.1007/s13391-012-2131-x

Effect of Synthesizing Method on the Properties of $LiFePO_4$/C Composite for Rechargeable Lithium-Ion Batteries

Man-Soon Yoon,[1] Mobinul Islam,[1] Young Min Park,[2] and Soon-Chul Ur[1,*]

[1]Department of Materials Sci. and Eng./Research Center for Sustainable Eco-Devices and Materials (ReSEM), Korea National University of Transportation, Chungju 380-702, Korea
[2]Research Institutes of Industrial Science and Technology, Fuel Cell Project, Pohang 790-330, Korea

(received date: 6 August 2012 / accepted date: 21 September 2012 / published date: March 2013)

Olivine-type $LiFePO_4$/C cathode materials are fabricated with $FePO_4$ powders that are pre-synthesized by two different processes from iron chloride solution. Process I is a modified precipitation method which is implemented by the pH control of a solution using NH_4OH to form $FePO_4$ precipitates at room temperature. Process II is a conventional precipitation method, of which H_3PO_4 (85%) solution is gradually added to a $FeCl_3$ solution during the process to maintain a designated mole ratio. The solution is subsequently aged at 90°C in a water bath until $FePO_4$ precipitates appear. In order to synthesize $LiFePO_4$/C composites, each batch of $FePO_4$ powders is then mixed with pre-milled lithium carbonate and glucose (8 wt. %) as a carbon source in a ball-mill. The structural characteristics of both $LiFePO_4$/C composites fabricated using iron phospates from two different routes have been examined employing XRD and SEM. The modified precipitation process is considered to be a relatively simple and effective process for the preparation of $LiFePO_4$/C composites owing to their excellent electrochemical properties and rate capabilities.

Keywords: lithium iron phosphate, composite material, amorphous material, precipitation, industrial waste

1. INTRODUCTION

Lithium iron phosphates have recently been given a great deal of attention as a positive electrode material in lithium batteries due to the low cost of constituent materials, the abundant resources of Fe and their environmental friendly nature.[1] For the synthesis of $LiFePO_4$, divalent Fe(II)-acetate or Fe(II)-oxalate, Li_2CO_3 and ammonium phosphate are generally utilized as starting materials.[1,2] However, divalent Fe(II)-acetate or Fe(II)-oxalate is relatively expensive and toxic. In contrast, Fe(III) salts are relatively less expensive and more stable,[2,3] so that overall manufacturing cost and safety may be optimized. Precipitation routes are widely used in synthesizing cathode materials, since they allow atomic level homogeneity when mixing the starting compounds, compared to conventional solid state approaches.[1] In addition, a wide range of low-cost reactants for the precipitation method are available. For example, iron chloride, iron nitrate and iron sulfate are successfully used, because Cl^-, NO_3^- and SO_4^{2-} can be readily dissolved into the solution and can also be easily removed.[4-7] The precipitation route is also a relatively simple scale-up process with low energy consumption in comparison to various other wet chemistry processes such as hydrothermal processing, sol-gel processing, spray pyrolysis, etc.[8-10]

Iron (III) phosphate has recently gained interest as a compatible source of both iron and phosphate in the field of lithium batteries.[11,12] Iron (III) phosphate can be prepared by a precipitation technique from aqueous solution.[11,12] Here, two possible precipitation processes can be considered for the synthesis of iron phosphates. First, a conventional process is followed using precursors in aqueous solution, in which precipitates can be formed through temperature control. The second process can be a modified process, for which pH control is adopted to facilitate the formation of desired precipitates. It has been shown that iron (III) phosphate prepared by a precipitation technique via temperature control results in micro-sized precipitate particles.[11] It shall also be speculated that corrosive HCl fume is frequently evolved during isothermal precipitation processes when using chloride salts. To avoid these complications, a modified precipitation route via pH control is considered.

Typically, ferric chloride ($FeCl_3$) solutions are by-products or waste streams of various manufacturing processes, including the pickling of steel scrap, of which $FeCl_3$ solution is waste liquid. $FeCl_3$ solution is also a by-product of titanium dioxide production. The major uses for $FeCl_3$ solution are municipal wastewater treatment and potable water treatment and in many different industrial applications. In water and waste water operations, ferric chloride is used as coagulants or flocculants, for odor control to minimize hydrogen sulfide

*Corresponding author: scur@ut.ac.kr

release, for phosphorus removal, and as a sludge thickening, conditioning and dewatering agent. The use of $FeCl_3$ in the electronics field is only a minor component.

The objectives of the present study are to develop an inexpensive and simple route for synthesizing iron phosphates from industrial by-product $FeCl_3$ and to investigate the process effect on the properties of subsequent lithium iron phosphates. For these purpose, olivine-type $LiFePO_4$/C cathode materials are fabricated with $FePO_4$ powders pre-synthesized by two different processes. This study provides useful process information on synthesizing iron phosphates and subsequent olivine-type $LiFePO_4$/C composites. $FeCl_3$ (38%) solution, which was used in this study as an iron source, is an industrial waste product and is the least expensive ($0.5/L) among all other iron sources. Synthesis of $LiFePO_4$/C composite by using this precursor with other low priced precursors such as H_3PO_4 and glucose is reported here for the first time. Two different precipitation methods for synthesizing $LiFePO_4$/C composite are highlighted in this study by using an inexpensive precursor $FeCl_3$ solution rather than focusing on their electrochemical properties.

2. EXPERIMENTAL PROCEDURE

2.1 Materials

The starting materials used for synthesizing amorphous $FePO_4$ were $FeCl_3$ solution (38%, AR), H_3PO_4 (85%, AR) solution and NH_4OH (25% - 30%, AR). Li_2CO_3 (99%, AR) and glucose (98%) were used with pre-synthesized $FePO_4$ for fabricating the $LiFePO_4$/C composite. The glucose and H_3PO_4 solution were purchased from Samchun pure chemical Co., Ltd., while Li_2CO_3 was purchased from SQM. The $FeCl_3$ solution was supplied by Dea Myoung Chemical. All the chemicals were used as received without further purification.

2.2 Synthesis of $LiFePO_4$/C composites

To synthesize olivine-type $LiFePO_4$/C cathode materials, $FePO_4$ powders prepared from two different processes were used. The first process is designated as process I, which was conducted by the pH control of solution using NH_4OH at room temperature in order to precipitate an iron phosphate identical to that used in a previous study,[12] but with different starting materials. The second process is designated as process II, for which the solution was isothermally maintained at 90°C until precipitates formed. For process II, the pH of the solution was in the range of 0.1 - 0.5 (imposed by H_3PO_4).

Step I: For process I, a certain amount of H_3PO_4 (85%) solution was gradually added drop wise to the $FeCl_3$ solution and stirred for 1 hour. NH_4OH was then slowly added to the solution to control the pH value with vigorous stirring at room temperature.

In order to compare the process effect, $FePO_4$ powders having the same composition as those in process I were synthesized in process II. For process II, a solution mixture was prepared with aqueous $FeCl_3$ salts and H_3PO_4 (85%) solution and the solution was stirred for 1 hour. The solution was subsequently aged at 90°C in a water bath until precipitates appeared. The white colored precipitates fabricated from processes I and II were then isolated by filtration, and washed with distilled water and isopropyl alcohol. After washing precipitates ($FePO_4{\cdot}xH_2O$), a drying process was carried out at 100°C for 6 hours. XRD analysis revealed that precipitates are of mostly an amorphous state.

Step II: $LiFePO_4$/C was synthesized by a solid state reaction process using pre-milled Li_2CO_3 and pre-synthesized amorphous $FePO_4{\cdot}xH_2O$ powders. Appropriate amounts of precursors and glucose (8 wt. %) were weighed and ball-milled with a ZrO_2 media in ethanol for 24 hours. The mixture was then dried at 80°C for 4 hours. The dried powders were then fired at 700°C for 4 hours under an N_2 atmosphere to prevent the oxidation of Fe^{2+} and to coat the surface of $LiFePO_4$ particles with carbon.

2.3 Structural characterization

To observe phase information and possible second phase formation in precursor states, the amorphous $FePO_4{\cdot}xH_2O$ powders were heat treated in air at 600°C - 700°C for 3 hours to obtain crystalline $FePO_4$ powders. Thermo gravimetric analysis (TGA) and differential scanning colorimetric analysis (DSC) were conducted using a thermal analysis system (NETZSCH 449C) with a heating rate of 10°C min^{-1}. The powder x-ray diffraction (XRD, Rigaku, D/MAX-2500H) analysis with Cu Kα radiation was used to identify the crystalline phases of the prepared materials. In order to observe the microstructures, e-SEM (FEI, Quanta-400) and FE-SEM (Jeol, JSM-6700F) were employed.

2.4 Electrochemical characterization

For electrochemical property assessment, electrodes were fabricated from a mixture of carbon coated $LiFePO_4$ powders (80 wt. %), carbon black (Super P, 10 wt. %), and polytetrafluoro ethylene (PTFE, 10 wt. %) as a binder in N-methyl-2-pyrrolidone (NMP) solution. This slurry was spread onto Al foil and dried in a vacuum at 120°C for 4 hours. Electrochemical properties were measured for coin cells (CR2016), which were assembled in a glove box under an Ar atmosphere. The electrolyte used was 1M $LiPF_6$ in a mixture of ethylene carbonate (EC) and dimethyl carbonate (DMC) (1 : 1 volume). The cells were galvanostatically charged and discharged at a voltage range of 1.8 - 4.2 V against the Li anode in a WONATECH (WBCS-3000) battery testing system at room temperature. CVs were measured on an impedance/electrochemical measurement system (IVIUMSTAT, Germany) with a scan rate of 0.1 mV s^{-1} between 2.6 and 4.2 V at room temperature.

3. RESULTS AND DISCUSSION

3.1 Phase analysis and powder morphology of $FePO_4$ precursor

To observe the dehydrating and phase transition temperature, TG/DSC analysis for the $FePO_4{\cdot}xH_2O$ synthesized by process I is performed and an exothermic peak appears at 568°C, indicating crystallization of amorphous $FePO_4$ to hexagonal $FePO_4$. Based on the analysis, $FePO_4{\cdot}xH_2O$ precursors are determined to calcine above 600°C and the phase information is investigated. XRD patterns for both iron phosphates heat-treated at 600°C and 700°C are presented in Figs. 1(a) and (b), respectively. All XRD patterns are fully stabilized to a hexagonal structure without second phase formation after heat treatment at 600°C. At 700°C, however, a second phase of $Fe_4(P_2O_7)_3$ appears in the iron phosphate synthesized from process II. In contrast, any secondary peaks are not observed in the iron phosphate fabricated by process I. From this x-ray analysis, the following reaction (simplified) can be speculated as:

Process I:

At room temperature:

$$FeCl_3\ (aq.) + H_3PO_4\ (aq.) + NH_4OH\ (aq.) \rightarrow FePO_4 \cdot xH_2O\downarrow + (NH_4)_3PO_4\ (aq.) + NH_4Cl\ (aq.) \quad (1)$$

Process II:

At 90°C:

$$FeCl_3\ (aq.) + H_3PO_4\ (aq.) \rightarrow FePO_4 \cdot xH_2O\downarrow + Fe_4(P_2O_7)_3 \cdot xH_2O\downarrow + HCl \quad (2)$$

As the temperature increases to 600°C, amorphous $FePO_4$ is transformed to the hexagonal crystal structure, while in the case of process II, the $Fe_4(P_2O_7)_3$ phase remains in an amorphous state. At a further increase of temperature to 700°C, the crystallization of $Fe_4(P_2O_7)_3$ occurs. This prediction for the chemical reaction in process II seems to coincide with the results of the x-ray analysis, as shown in Fig. 1(b). Similarly, Marasinghe *et al.*[13] reported that $Fe_4(P_2O_7)_3$ started to crystallize at 700°C in an iron phosphate glass system. Thus, the observed secondary peaks at 700°C in Fig. 1(b) indicate the existence of crystallized $Fe_4(P_2O_7)_3$ in $FePO_4$. This is referred to at the JCPDS card number 360318. Considering the fact that the secondary peak appears only in process II, the elevated temperature in the process may play a role in the second phase formation.

Morphologies of iron phosphates synthesized by processes I and II are presented in Figs. 2(a) and (b), respectively. Comparing these processes, it can be seen that process I results in a reduced particle size along with homogeneity, while process II shows a relatively larger particle size with an irregular shape. The average particle size of the iron phos-

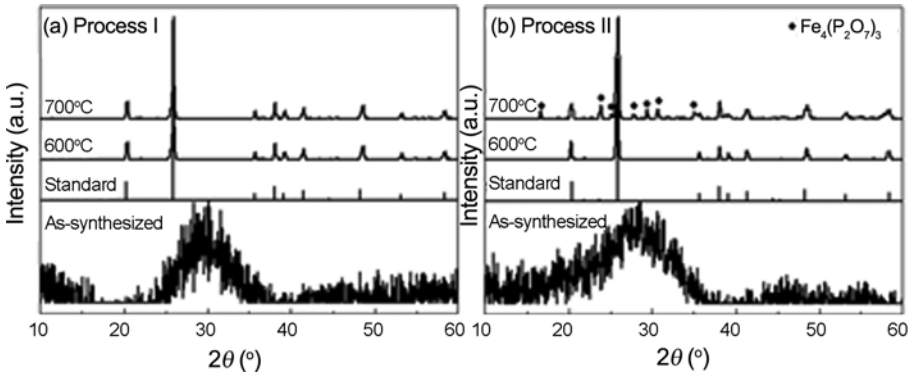

Fig. 1. XRD patterns of $FePO_4$ before and after heat treatments; (a) synthesized by process I and; (b) synthesized by process II.

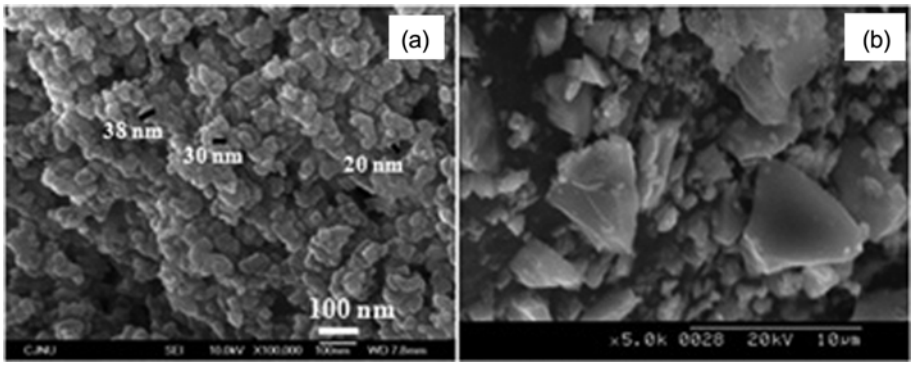

Fig. 2. SEM micrographs of as-synthesized $FePO_4$; (a) by process I and; (b) by process II.

phate synthesized by process I is about 30 nm with a sphere shape, whereas that by process II has a broader particle size distribution. It has been previously reported that the particle size and shape of iron phosphates increased and became more irregular under the lower pH and at a higher reaction temperature in a conventional precipitation process.[14] Reminding again To reiterate, process I is carried out at room temperature while maintaining the pH of 2.1, while process II is carried out at 90°C while the pH of the solution is in the range of 0.1 - 0.5. Therefore, it can be expected that the slightly higher pH and lower reaction temperature reduce particle size, even down to the nano-scale, and increase uniformity.

3.2 The crystal structure and powder morphology of $LiFePO_4$/C cathode materials

Before synthesizing the $LiFePO_4$/C composite, lithium carbonate is milled in advance in a high energy nano-mill to effectively eliminate possible problems associated with size and shape differences and to enhance the reaction activities in starting materials. The SEM micrographs of as-received and pre-milled Li_2CO_3 powders are presented in Fig. 3. It can be seen that the pre-milling process results in reduced particle size and enhances the reaction activities with precursors.

The XRD patterns of heat-treated $LiFePO_4$/C composites, which are fabricated with pre-synthesized $FePO_4 \cdot xH_2O$ and pre-milled Li_2CO_3, are shown in Fig. 4. The $LiFePO_4$/C composite fabricated with the iron phosphate from process I reveals a single orthorhombic phase, whereas a secondary $Fe_2P_2O_7$ phase is observed in the $LiFePO_4$/C composite fabricated with the iron phosphate from process II. The second phase is similar to that observed in Fig. 1(b). As mentioned, the $FePO_4 \cdot xH_2O$ precursor from process II contains $Fe_4(P_2O_7)_3$ after heat-treating at 700°C in air. Consequently, it can be considered that $LiFePO_4$/C composites are heat-treated with a reducing agent of a carbon source under an N_2 atmosphere so that Fe^{3+} can be reduced to Fe^{2+}, leading to the $Fe_2P_2O_7$ formation in the composite.

SEM micrographs of $LiFePO_4$/C composites fabricated

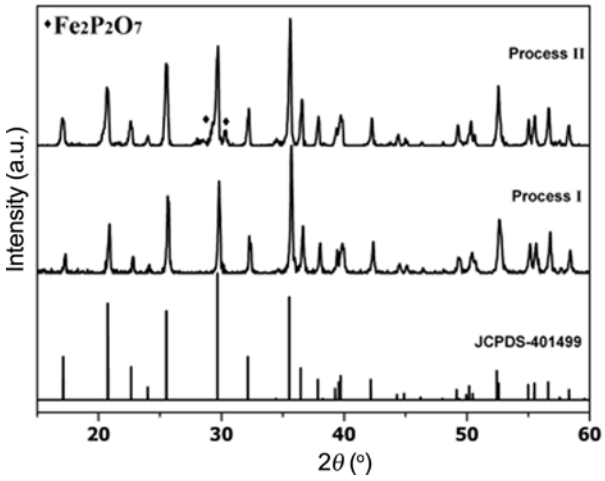

Fig. 4. XRD patterns of $LiFePO_4$/C composites fabricated with the pre-synthesized $FePO_4$ from two different routes.

with iron phosphates from process I and II (designated as samples A and B, respectively) reveal the influence of the synthesis method on particle size before heat treatment as shown in Figs. 5(a) and (b), respectively, and those after heat treatment as shown in Figs. 5(c) and (d), respectively. As shown in Figs. 5(a) and (b), sample A has an average particle size of ~30 nm with a near spherical and narrow size distribution, but some agglomerations are shown. In contrast, sample B particles are irregular shaped with broad particle size distribution and less agglomeration. After heat treatment, particle sizes in sample A increases somewhat, while those in sample B exhibit a restricted growth with a bimodal size distribution. The particle growth in sample A can be speculated in two ways. The first speculation can be the effect of agglomeration, which inhibits carbon sources from diffusing deep inside the agglomerates. In this study, carbon source, which is known to prohibit the particle growth during heat treatment,[15-17] is believed to be coated only on the surface of agglomerates. The second speculation can be the nano size effect. Surface area is considerably increased in

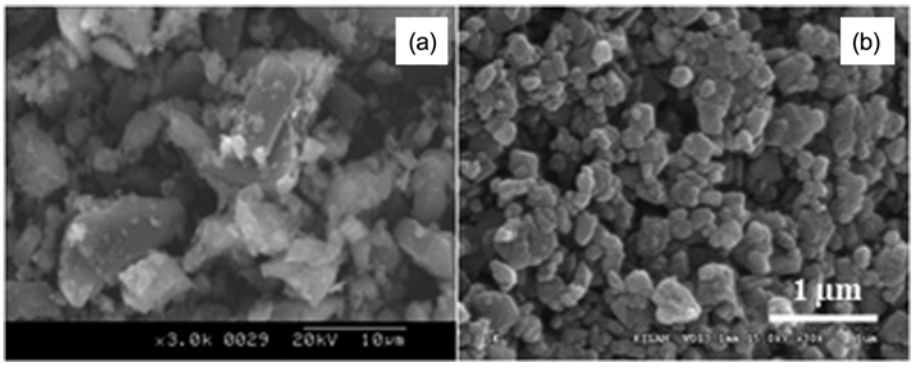

Fig. 3. SEM micrographs of Li_2CO_3; (a) as-received and; (b) nano-milled.

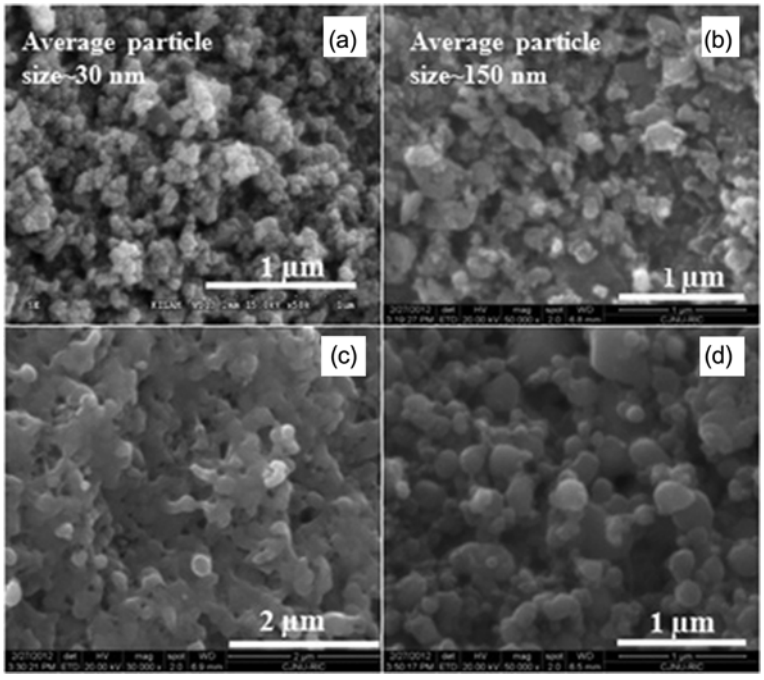

Fig. 5. SEM micrographs of $LiFePO_4$/C composites; (a) fabricated with the pre-synthesized $FePO_4$ by process I, before heat treatment; (c) as for (a), but after heat treatment; (b) fabricated with the pre-synthesized $FePO_4$ by process II, before heat treatment, and; (d) as for (b), but after heat treatment.

nano sized particles, and hence can provide a driving force for the particle growth.[18] Since particles in sample B are relatively well dispersed, the carbon source seems to be rather uniformly coated on the surface of individual particles, possibly leading to the retardation of particle growth.

3.3 Electrochemical properties

3.3.1 Charge/discharge and cyclic performances

Figure 6 presents the charge/discharge voltage profiles and cyclic performances of sample A and B electrodes. The initial charge and discharge capacity of sample A are 157 and 136 $mAhg^{-1}$, respectively. For sample B, the charge capacity is 110 $mAhg^{-1}$, and the discharge capacity is 88 $mAhg^{-1}$. Sample A exhibits a flat charge/discharge plateau around 3.47 and 3.40 V, and that for sample B is around 3.5 and 3.37 V, implying that redox reaction occurs between the $FePO_4$ and $LiFePO_4$ phases. Sample A has a relatively higher charge/discharge capacity compared to sample B. This can be ascribed to the presence of a single orthorhombic phase without existence of any second phases, despite the relatively larger particle size and poor carbon coating in sample A. From the discussions above, it can be considered that a second phase in $LiFePO_4$ seems to take precedence in the decrease of specific capacity over particle size and carbon coating quality. Both samples show excellent cyclic behavior even after 30 cycles. This in turn suggests that a second phase is closely related to the decrease in specific capacity, but has no specific influence on the cyclic performance in this study. There could be an opportunity to optimize particle size and appropriate percentage of carbon for coating, which may lead to enhance the electrochemical property.

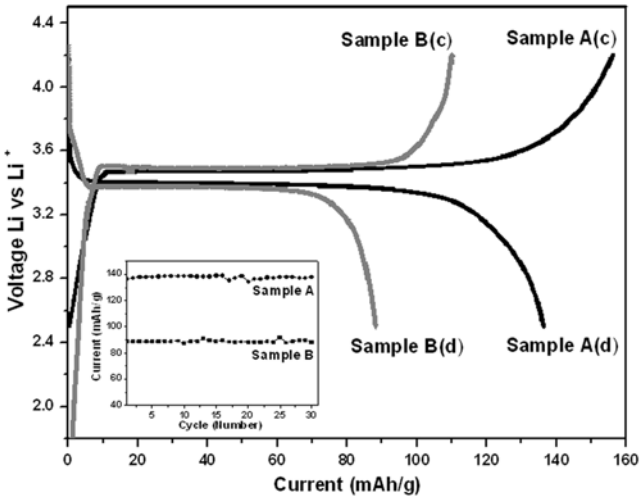

Fig. 6. Initial charge(c)-discharge(d) curves of lithium cells with $LiFePO_4$/C fabricated by two different routes at a current rate of 0.1C. Inset: Discharge cyclic performance of lithium cells with $LiFePO_4$/C fabricated by two different routes.

3.3.2 Cyclic voltammogram

Typical cyclic voltammograms of $LiFePO_4$ (samples A

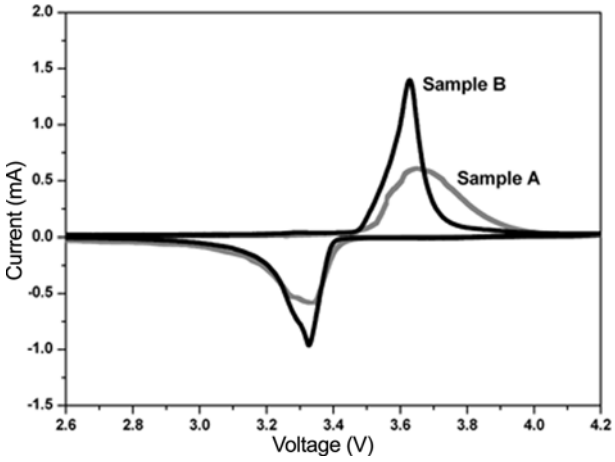

Fig. 7. Cyclic voltammograms of lithium cell with $LiFePO_4$/C fabricated by two different routes.

and B) cathode materials are provided in Fig. 7. Here, the lithium foil acts as counter and reference electrodes. The cyclic voltametric curves indicate that intercalation/disintercalation occurs within the potential range and the phase transition, if there is one, seems to proceed during the process. Sample A and B cathodes show single anodic peaks at 3.65 and 3.63 V, respectively, during the charge cycle. This corresponds to the single-step lithium-ion removal from cathode materials. Single cathodic peaks are obtained at 3.34 and 3.33 V for samples A and B, respectively, which correspond to the Li^+ reinsertion into cathodes. The cyclic voltammetry curve for sample B shows a relatively symmetrical and sharper shape in both charge and discharge runs, compared to sample A. Stronger and sharper peaks in sample B intuitively indicate the enhancement of the lithium-ion diffusion, possibly due to the relatively smaller particle size and uniformly coated carbon, as presented in Fig. 5(d). The peak potential difference (ΔE_p) between anodic and cathodic peaks is 0.31 V in sample A, whereas that in sample B is 0.3 V. This indicates that both cathode samples have a similar reversible/quasi-reversible nature of the Li^+ transport behavior in the electrochemical cell between the $LiFePO_4$ and $FePO_4$ structures.

4. CONCLUSIONS

A simple route for synthesizing iron phosphates is suggested and the process effect on the properties of subsequent $LiFePO_4$/C is systematically investigated in this study. Results reveal that iron phosphate particles prepared from a modified precipitation process (process I) are in the range of 20 - 50 nm, whereas those of iron phosphates prepared from a conventional precipitation process (process II) are relatively larger and more irregularly shaped. Process I ensures the formation of a single phase olivine structure without any second phases, while a secondary $Fe_2P_2O_7$ phase exists in the $LiFePO_4$/C composites prepared in process II. Through electrochemical property measurements, significant improvements in the initial charge/discharge capacity are observed in the $LiFePO_4$/C composites fabricated with the iron phosphates from process I. The decreased charge/discharge capacity in the $LiFePO_4$/C composites fabricated with the iron phosphates from process II can possibly be ascribed to the existence of the second phase $Fe_2P_2O_7$. However, both samples show excellent cyclic behavior even after 30 cycles. A second phase $Fe_2P_2O_7$ in the composite seems to take precedence in the decrease of specific capacity over particle size and carbon coating quality, but has no specific influence on the cyclic performance in this study. In addition, evolution of noxious HCI fumes can be successfully evaded by process I. Therefore, the modified precipitation process is considered to be a relatively uncomplicated and effective process for the preparation of $LiFePO_4$/C composites owing to their excellent electrochemical properties and rate capabilities.

ACKNOWLEDGEMENTS

The research was supported by a grant from the Regional Innovation Center (RIC) Program which was conducted by the Ministry of Knowledge Economy of the Korean Government.

REFERENCES

1. D. Jugovic and D. Uskokovic, *J. Power Sources* **190**, 538 (2009).
2. C. M. Julien, A. Mauger, and K. Zaghib, *J. Mater. Chem.* **21**, 9955 (2011).
3. S. Okada, T. Yamamoto, Y. Okazaki, J. Yamaki, M. Tokunaga, and T. Nishida, *J. Power Sources* **146**, 570 (2005).
4. S. Yang, P. Y. Zavalij, and M. S. Whittingham, *Electrochem. Commun.* **3**, 505 (2001).
5. J. Ying, M. Lei, C. Jiang, C. Wan, X. He, J. Li, L. Wang, and J. Ren, *J. Power Sources* **158**, 543 (2006).
6. M. Konarova and I. Taniguchi, *Powder Technol.* **191**, 111 (2009).
7. C. Xu, J. Lee, and A. S. Teja, *J. Supercrit. Fluids* **44**, 92 (2008).
8. G. Arnold, J. Garche, R. Hemmer, S. Strobele, C. Vogler, and A. W. Mehrens, *J. Power Sources* **119-121**, 247 (2003).
9. K. Shiraishi, K. Dokko, and K. Kanamura, *J. Power Sources* **146**, 555 (2005).
10. M. H. Lee, J. Y. Kim, and H. K. Song, *Chem. Commun.* **46**, 6795 (2005).
11. Z. Liu, X. Zhang, and L. Hong, *J. Appl. Electrochem.* **39**, 2433 (2009).
12. Y. Lan, X. Wang, J. Zhang, J. Zhang, Z. Wu, and Z. Zhang,

Powder Technol. **212**, 327 (2011).
13. G. K. Marasinghe, M. Karabulut, C. S. Ray, D. E. Day, M. G. Shumsky, W. B. Yelon, C. H. Booth, P. G. Allen, and D. K. Shuh, *J. Non-Crystalline Solids* **222**, 144 (1997).
14. C. Delacourt, C. Wurm, M. Morcrette, and C. Masquelier, *J. Chem. Mater.* **15**, 5051 (2003).
15. Y. Lin, M. X. Gao, D. Zhu, Y. F. Liu, and H. G. Pan, *J. Power Sources* **184**, 444 (2008).
16. S. A. Needham, A. Calka, G. X. Wang, A. Mosbah, and H. K. Liu, *Electrochem. Commun*. **8**, 434 (2006).
17. L.-L. Xie, K.-Q. You, X.-Y. Cao, C.-F. Zhang, D.-W. Song and L.-B. Qu, *Electron. Mater. Lett*. **8**, 411 (2012).
18. M. M. Rashad and M. I. Nasr, *Electron. Mater. Lett*. **8**, 325 (2012).